Featured in Physics

Kinematic Signatures of Impulsive Supernova Feedback in Dwarf Galaxies

Jan D. Burger*
Department of Physics and Astronomy, University of California, Riverside, California 92521, USA; University of Iceland, Dunhagi 5, 107 Reykjavík, Reykjavíkurborg, Iceland; and Max-Planck-Institut für Astrophysik, Karl-Schwarzschild-Str. 1, 85748 Garching, Bayern, Germany

Jesús Zavala
University of Iceland, Dunhagi 5, 107 Reykjavík, Reykjavíkurborg, Iceland

Laura V. Sales
Department of Physics and Astronomy, University of California, Riverside, California 92521, USA

Mark Vogelsberger
MIT Kavli Institute for Astrophysics and Space Research, Ronald McNair Building, 37-611, Cambridge, Massachusetts 02139, USA and The NSF AI Institute for Artificial Intelligence and Fundamental Interactions, Massachusetts Institute of Technology, 77 Massachusetts Ave, Cambridge, Massachusetts 02139, USA

Federico Marinacci
Department of Physics and Astronomy "Augusto Righi", University of Bologna, Bologna, I-40129, Italy

Paul Torrey
Department of Astronomy, University of Florida, 211 Bryant Space Sciences Center, Gainesville, Florida 32611, USA

(Received 22 August 2021; revised 6 June 2022; accepted 9 September 2022; published 1 November 2022)

Impulsive supernova feedback and nonstandard dark matter models, such as self-interacting dark matter (SIDM), are the two main contenders for the role of the dominant core formation mechanism at the dwarf galaxy scale. Here we show that the impulsive supernova cycles that follow episodes of bursty star formation leave distinct features in the distribution function of stars: groups of stars with similar ages and metallicities develop overdense shells in phase space. If cores are formed through supernova feedback, we predict the presence of such features in star-forming dwarf galaxies with cored host halos. Their systematic absence would favor alternative dark matter models, such as SIDM, as the dominant core formation mechanism.

DOI: 10.1103/PhysRevLett.129.191103

Introduction.—One of the most persevering small-scale challenges [1] to the collisionless cold dark matter (CDM) paradigm concerns the inner density profiles of dark matter (DM) halos that host dwarf galaxies. Hints for constant density cores observed in some dwarf galaxies [2–7] appear to be at odds with the ubiquitous cusps predicted by CDM N-body simulations [8,9]. To reconcile the success of the CDM paradigm at predicting the properties of the large-scale structure of the Universe with these observations on the scale of low-mass galaxies, a physical mechanism is required to remove the central DM cusps predicted by CDM N-body simulations [8,9]. A potential way to flatten the central density profile of halos is through strong and impulsive fluctuations in the gravitational potential caused by supernova-driven episodes of gas removal [10–16]. For supernova feedback (SNF) to be effective, supernovae must occur in quasiperiodic cycles and cause strong fluctuations in the central potential on timescales that are shorter than the typical dynamical time in the galaxy, i.e., impulsively [11]. As the time between the birth of a heavy ($\gtrsim 8\ M_\odot$) star and its type II supernova explosion is less than $\sim$40 Myrs, such quasiperiodic SN cycles can only be realized in galaxies with a bursty star formation history, i.e., a star formation rate that shows order of magnitude fluctuations over less than a dynamical time (see Ref. [17] for a similar definition of "bursty"). Although there is evidence of bursty star formation in dwarf galaxies at the high mass end [18], the duration of star bursts in the intermediate- and low-mass regime is far more uncertain [19,20]. In cosmological simulations, SNF is most efficient at forming cores on the scale of bright dwarfs [12–14], as long as the simulated star formation history is bursty and the gas dominates the binding energy in the inner halo before being expelled by feedback, causing a strong fluctuation in the total potential [15,17].

In modern subresolution models of the interstellar medium (ISM, e.g., Refs. [21,22]), both the (average)

burstiness of star formation and the maximal densities to which gas cools before forming stars can be regulated via a single numerical parameter set at the resolved scales in the simulations, the so-called star formation (SF) threshold $n_{\rm th}$, which gives the minimum density that gas needs to reach before it is eligible to form stars [15]. In an otherwise fixed, idealized (noncosmological) setup, adopting larger values of $n_{\rm th}$ results in burstier SF, more substantial potential fluctuations, and thus more impulsive SNF, until eventually a threshold for core formation is reached (see Ref. [16] for a discussion).

An adiabatic way to form a core is through elastic scattering between DM particles. Self-interacting DM (SIDM, [23–26]) redistributes energy from the outside in, leading to the formation of a ∼1 kpc size DM core in dwarf-size halos, provided the self-interaction cross section is $\sigma_T/m_\chi \sim 1\ {\rm cm}^2\,{\rm g}^{-1}$ on the scales of dwarf galaxies [24,27,28]. Such value of the cross section also evades current constraints [29–31], while for cross sections smaller by about 1 order of magnitude, SIDM is indistinguishable from CDM [32]. Contrary to SNF, SIDM causes the formation of cores in all haloes below a certain mass, and thus, observations of dwarf galaxies with cuspy host haloes (e.g., Ref. [31]) are more challenging to explain in SIDM (however, see Ref. [33] for a possible explanation).

In this Letter we use a suite of hydrodynamical simulations of an isolated dwarf galaxy to demonstrate that impulsive SNF produces distinct, shell-like kinematic signatures that appear in the phase space distribution of stars in dwarf galaxies—and argue that the systematic absence of such features across star-forming dwarf galaxies with confirmed cores, and in particular in dwarfs with recent starbursts, would point to an adiabatic core formation mechanism, such as SIDM.

Simulations.—The results presented here are derived from a suite of 16 high-resolution (with a DM particle mass $m_{\rm DM} \sim 1.3 \times 10^3\ {\rm M}_\odot$ and a typical baryon mass $m_b \sim 1.4 \times 10^3\ {\rm M}_\odot$, shown in Sec. IA of the Supplemental Material [34]) simulations of an isolated dwarf galaxy with a total baryonic mass of $M_b = 7.2 \times 10^8\ {\rm M}_\odot$ and structural properties similar to those of the small Magellanic cloud (see Refs. [21,22,34,47]). We use the formalism described in Ref. [48] to generate the initial conditions of a system in approximate hydrostatic equilibrium.We then simulate the evolution of the isolated system, using the ISM model SMUGGLE [22] for the cosmological simulation code AREPO [49], along with the SIDM model presented in Ref. [24], for 16 different combinations of the star formation threshold $n_{\rm th}$ and the SIDM self-interaction cross section σ_T/m_χ. In Fig. 1, we demonstrate that nearly identical constant density DM cores can form adiabatically in SIDM simulations with smooth star formation histories (low values of $n_{\rm th}$) and $\sigma_T/m_\chi \sim 1\ {\rm cm}^2\,{\rm g}^{-1}$ and through impulsive SNF in CDM simulations with bursty star formation histories (high values of $n_{\rm th}$). While identical cores can form through SIDM and impulsive SNF, the phase space distribution of baryons is distinctly different between simulations with or without impulsive SNF, irrespective of whether DM is self-interacting. Hereafter, we illustrate this difference by comparing the results of the CDM runs with $n_{\rm th} = 0.1\ {\rm cm}^{-3}$ (representative of smooth SF and thus adiabatic SNF) and $n_{\rm th} = 100\ {\rm cm}^{-3}$ (representative of bursty SF and thus impulsive SNF).

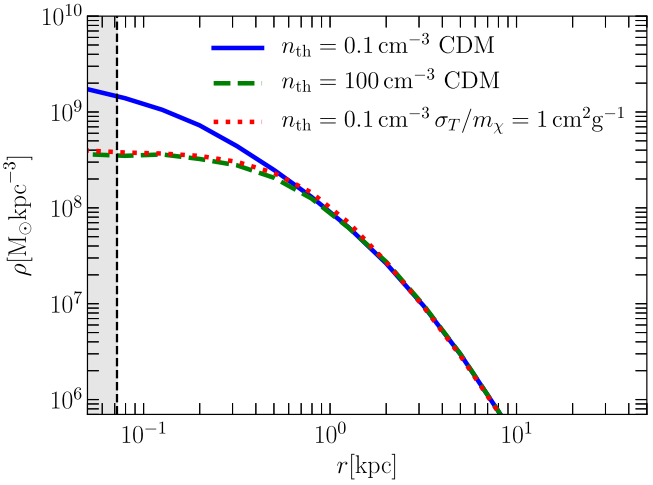

FIG. 1. Adiabatic and impulsive cusp-core transformation: Spherically averaged radial DM density of three different simulated dwarf-size halos after 3 Gyr of simulation time. The solid blue line corresponds to the CDM simulation with smooth star formation ($n_{\rm th} = 0.1\ {\rm cm}^{-3}$), whereas the dashed green line denotes the result of the CDM simulation with bursty star formation ($n_{\rm th} = 100\ {\rm cm}^{-3}$). The red dotted line corresponds to the SIDM simulation with smooth star formation ($n_{\rm th} = 0.1\ {\rm cm}^{-3}$) and a self-interaction cross section $\sigma_T/m_\chi = 1\ {\rm cm}^2\,{\rm g}^{-1}$.

Projections of the gas distribution after 3 Gyr of simulation time are shown in Fig. 2 for both benchmark simulations. The gas distributions of the two runs look strikingly different, in particular toward the center of the galaxies. In the simulation with bursty SF—and thus with impulsive SNF—the central gas density is lower than in the immediate surroundings due to a supernova-driven gas outflow extending out of the galactic disc, which can be clearly appreciated as a nearly spherical bubble in the edge-on projection. In contrast, in the simulation with smooth SF, the edge-on projection of the gas appears rather regular, and the face-on projection has no distinct features.

Stellar phase space shells.—Figure 3 shows (for both benchmark CDM runs) the metallicity distribution and the mass-weighted distribution function of mono-age stars which are 0.8–0.9 Gyr old projected onto the $R - v_R$ plane at the end of the simulation. For the simulation with smooth SF, we observe a steady decrease of the average metallicity of stars with an increasing cylindrical radius, a natural

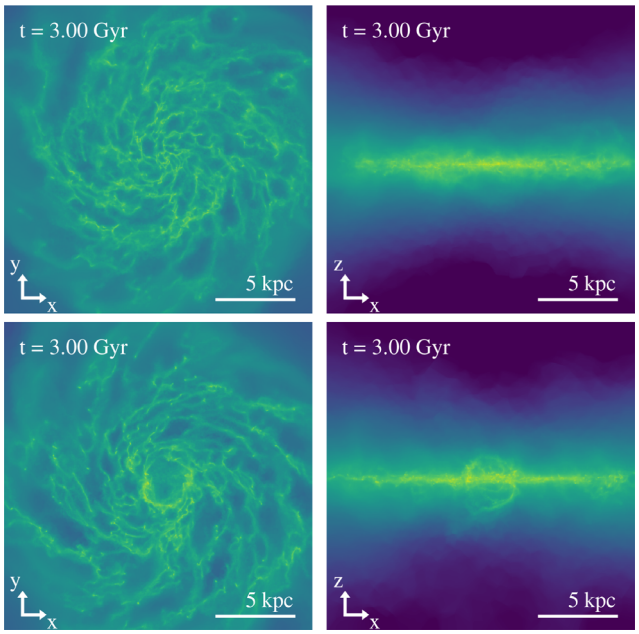

FIG. 2. Gas distributions of resulting galaxies after 3 Gyr of simulation time for two simulations with different star formation thresholds. We show face-on (left column) and edge-on (right column) projections of the gas density for the CDM simulation with smooth (top row) and bursty (bottom row) star formation. The side length of the field of view is 20 kpc in each panel, and we defined a coordinate system such that the z axis is perpendicular to the gas disc. Notice how central gas is vertically expelled out of the disc plane in the simulation with bursty star formation. Such galactic outflows are characteristic of violent and impulsive events of supernova-driven energy release.

consequence of the centrally concentrated star-forming gas. Statistically, more stars form in environments with higher gas densities, i.e., toward the center of galaxies. Thus, the subsequent SNF cycles cause a metal enrichment of the ISM that is larger in the central regions. Therefore, stars of subsequent generations (like the ones shown in Fig. 3) acquire a negative metallicity gradient. Moreover, the radial velocities of stars are rather small in magnitude, $v_R \sim 25\ \mathrm{km\,s^{-1}}$ at most. A different picture emerges in the center of the galaxy with impulsive SNF. Instead of a monotonic stellar metallicity gradient, a pattern of several shells in $R - v_R$ space emerges in the metallicity distribution—and the mass-weighted distribution function—of stars with similar ages. The shells are composed of star particles with high metallicities, some of which move at radial speeds of more than $50\ \mathrm{km\,s^{-1}}$. These high-metallicity shells intersect phase space regions inhabited by more metal-poor star particles whose radial speeds are smaller on average. Such features are transient for a given group of stars, but occur at various times in the evolution, and are not unique to the CDM run with $n_{\mathrm{th}} = 100\ \mathrm{cm^{-3}}$; we find them also in other simulations (both in CDM and SIDM), as long as the SF histories in these simulations are bursty—and SNF is impulsive. For our choice of initial conditions and fixed SMUGGLE parameters, the transition from smooth to bursty SF—and thus to impulsive SNF—happens around $n_{\mathrm{th}} = 10\ \mathrm{cm^{-3}}$ (see Ref. [16]). Notice that shells appear in all simulations in which SNF is impulsive—regardless of whether the DM is self-interacting or not.

To quantify the difference between the final stellar distributions in the bursty SF case and in the smooth SF case shown in Fig. 3, we estimate the likelihood of randomly finding, in the smooth SF case, an overdensity similar to that associated with the clear shell in the bursty SF simulation. We take the normalized, cumulative stellar mass distribution of the smooth SF simulation as a target distribution for random sampling and construct 10^7 resampled distributions, each time drawing as many radii as there are stars in the original distribution. For each resampled distribution, we then search a predefined "signal area" for the largest spherical overdensity that arises as a result of Poisson sampling, as shown in Sec. ID of the Supplemental Material [34]. We also calculate the overdensity at the position of the shell in the bursty SF simulation. From these values, we create a distribution of global (signal region) and local (shell area) overdensities. Comparison against the measured shell overdensity in the bursty SF simulation reveals that the shell has a global (local) significance of more than 5σ (3.3σ) compared to the smooth SF case. These are conservative estimates for the significance of the shell-like feature since they are based on the stellar density distribution only and do not take into account information on the metallicity of stars. Finding an overdensity of such amplitude, combined with the observation that the overdensity consists mainly of high-metallicity stars, would be a smoking gun signature of an impulsive SNF cycle following an episode of bursty SF.

To determine how the shell-like features appear in the line-of-sight phase space of galaxies that are observed edge on, we projected the distributions shown in Fig. 3 into $|x| - v_y$ space (using the coordinate system defined in Fig. 2 [34]; see also Fig. 3 and Sec. IC in the Supplemental Material [34]). In the featureless smooth SF case, the emerging distribution of stars tracks the rotation curve of the galaxy, with a monotonic decrease of (average) metallicity with distance. In the bursty SF case, we observe two isolated overdense clusters consisting mainly of high-metallicity stars, at a distance to the galaxy's centre of $\sim$2 kpc, similar to the radius at which the phase space shell appears in Fig. 3. We explicitly confirmed that those clusters consist of the same stars as the phase space shell.We emphasize again that similar differences between the phase space distributions of stellar particles in galaxies with or without impulsive SNF emerge when SIDM simulations are considered.

How shells are created.—The shell-like features shown in Fig. 3 arise in the aftermath of starburst events—which are closely followed by impulsive episodes of SNF.

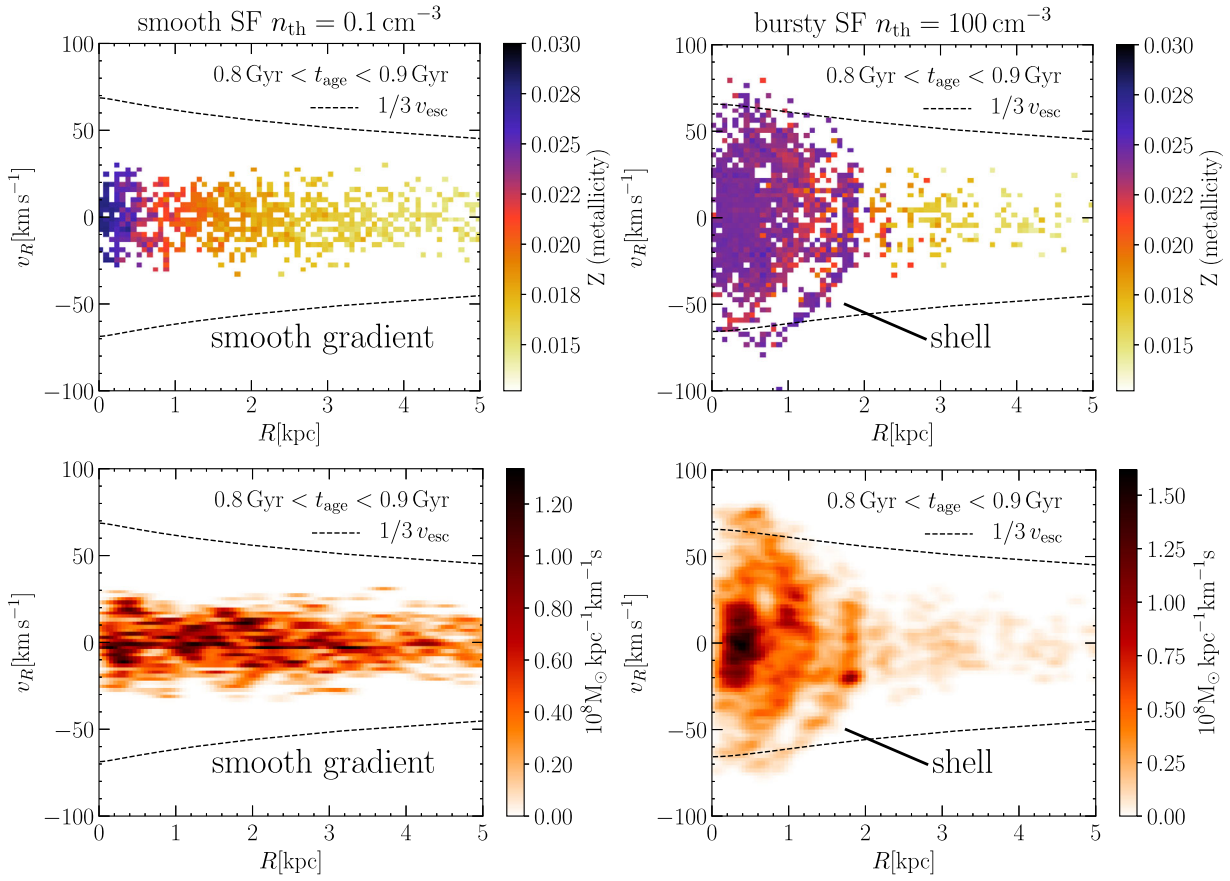

FIG. 3. Average metallicity distribution (top panels) and mass-weighted distribution function (bottom panels) of star particles calculated after 3 Gyr of simulation time for two different simulations, projected into the radial phase space ($R - v_R$). Star particles are subject to a cut in stellar age; only stars which are 0.8–0.9 Gyr old are shown in these plots. Averaged stellar metallicity (mass-weighted distribution function) is color coded according to the scale on the right of each panel. For scale, we show a third of the escape velocity as a function of radius as black dashed lines. The left (right) column corresponds to the CDM simulation with smooth (bursty) star formation. Smooth star formation results in a smooth metallicity gradient with the more enriched starts in the center. Bursty star formation results in an overall weaker gradient, along with the presence of a shell of stars with high metallicity that intersects a low metallicity population at $R \sim 2$ kpc. This shell appears as a distinct overdense region in the mass-weighted distribution function.

Reference [50] showed that young stars born in a turbulent ISM inherit the orbits of the star-forming gas and can be born with significant radial motion. The orbits of these stars are then further heated by subsequent feedback episodes, leading to sustained radial migration. The shells presented here form from such groups of stars, which are born during starburst events in a turbulent ISM. Such groups of stars constitute *orbital families* [16,51]—sets of orbits defined by similar integrals of motion (see Sec. II of the Supplemental Material [34]). Moreover, they are born with similar metallicities and—as outlined above—with some initial amount of radial motion.

Instead of causing a coherent net expansion, subsequent impulsive fluctuations in the gravitational potential discontinuously change the (gravitational) energy of a star (particle) by an amount that depends on its orbital phase [11,51]. As a consequence, they can split an initially phase mixed *orbital family*, i.e., create a distribution that is unmixed [16]. The phase space shells we observe are therefore signatures of the early stages of phase mixing [52,53]. To compare this to the smooth case, we note that in dynamical systems in which orbits are regular and stars act as dynamical tracers of the gravitational potential, the average metallicity of stars can only depend on their actions [54]. We can therefore generally assume *orbital families* to be well approximated by groups of stars with similar ages and metallicities. Across our simulation suite, we find that in simulations with impulsive SNF (following bursty SF), the energy distribution of *orbital families* is wider than in simulations with smooth SF (see Fig. 6 and Sec. IC in the Supplemental Material [34]), a direct result of the periodic, SNF-driven heating of stellar orbits (see Ref. [51]). The shell-like signatures of early-stage phase mixing observed here are thus a direct consequence of impulsive SNF.

Discussion and outlook.—Finding stellar shells similar to the ones presented here in nearby dwarfs would imply a prior episode of impulsive SNF without necessarily

establishing SNF as the dominant core formation mechanism. In cosmological halos, we expect that diffusion caused by the halo's triaxial shape will erase the shells within ∼1 dynamical time [51], implying that galaxies without recent bursty star formation (e.g., quenched galaxies) are fairly bad targets to look for phase space shells. Nevertheless, it is instructive to evaluate the potential of detecting such signatures of bursty SF in the Milky Way satellites, in particular Fornax [55–57], since it has been claimed to have a core [5] (albeit this remains controversial; see Ref. [58]), and information on line-of-sight kinematics, metallicity [55], and age [56] is available for a subsample of its member stars. Unfortunately, we find that the ages of individual stars carry uncertainties which are too large (∼1 Gyr) to conclusively identify *orbital families*. Ideal future targets to look for impulsive SNF signatures are star-forming field dwarfs in the vicinity of the Local Group (see Ref. [4]). At the current time, the number of resolved stars with known ages and metallicities in these galaxies is too small. Within the next decade, however, the Roman Space Telescope will provide precise photometric data of individual stars in dwarf galaxies within the local volume (e.g., [59]). Combined with spectroscopic data from the ground, this will enable the precision needed to determine the ages, metallicities, and kinematics of a sufficient number of stars to conclusively establish whether the characteristic shell-like signatures of impulsive SNF presented here—or rather their projections into the space of line-of-sight velocity vs projected radius (see Fig. 3 in the Supplemental Material [34])—are ubiquitously present or systematically absent. Further in the future, new generations of extremely large telescopes may even provide sufficiently precise data on the 3D motions of stars in nearby dwarfs to allow for a search of shells directly in $R - v_R$ space [60].

The significance of a (potential) nondetection of such shells in dwarf galaxies with a core also depends on how robust our results are to changes in the initial setup or the stellar evolution model. Apart from the host halo's triaxiality, two effects that we do not explicitly test for may be significant. First, SF histories in real dwarf galaxies may be bursty, but starbursts may occur away from the galaxy's center. However, SNF needs to impulsively change the central potential to be a feasible core formation mechanism (see Refs. [11,16]). The nondetection of kinematic signatures would then require starbursts to occur mainly in the center of dwarfs, but exclusively off center at late times, a possible but unlikely scenario (see Ref. [50]). Second, stellar clusters (i.e., *orbital families*) born in starburst events need to contain a sufficient number of stars to allow us to identify shells formed from them. Based on our resampling routine, as shown in Sec. ID of the Supplemental Material [34], we estimate that a shell needs to contain a few hundred stars to be significant at a 2σ level [notice that this implies that future experiments need to provide precise age and metallicity information for $\mathcal{O}(10^4)$ stars if we assume a constant average SF rate]. In a detailed high-resolution study of the impact of different kinds of stellar feedback, Ref. [61] found that clusters of such size formed in all simulations in which SNF was included. At this time, we are unaware of any study in which no clusters of at least ∼100 stars form, while SNF is modeled self-consistently and found to be a feasible core formation mechanism.

We thus infer that the conclusive, systematic absence of signatures of impulsive SNF across all isolated, star-forming field dwarfs with confirmed cores would give strong support to alternative DM models, such as SIDM.

J. B. and J. Z. acknowledge support by a Grant of Excellence from the Icelandic Center for Research (Rannís; Grants No. 173929 and No. 206930). The simulations presented here were carried out on the Garpur supercomputer, a joint project between the University of Iceland and University of Reykjavík with funding from Rannís. L. V. S. is grateful for financial support from Grants No. NASA ATP 80NSSC20K0566, No. NSF AST 1817233, and No. NSF CAREER 1945310. P. T. acknowledges support from NSF Grants No. AST-1909933 and No. AST-2008490, and NASA ATP Grant No. 80NSSC20K0502. F. M. acknowledges support through the program "Rita Levi Montalcini" of the Italian MUR.

*burger@mpa-garching.mpg.de

[1] J. S. Bullock and M. Boylan-Kolchin, Small-scale challenges to the ΛCDM paradigm, Annu. Rev. Astron. Astrophys. **55**, 343 (2017).
[2] B. Moore, Evidence against dissipation-less dark matter from observations of galaxy haloes, Nature (London) **370**, 629 (1994).
[3] R. Kuzio de Naray, S. S. McGaugh, and W. J. G. de Blok, Mass models for low surface brightness galaxies with high-resolution optical velocity fields, Astrophys. J. **676**, 920 (2008).
[4] J. I. Read, M. G. Walker, and P. Steger, Dark matter heats up in dwarf galaxies, Mon. Not. R. Astron. Soc. **484**, 1401 (2019).
[5] M. G. Walker and J. Peñarrubia, A method for measuring (slopes of) the mass profiles of dwarf spheroidal galaxies, Astrophys. J. **742**, 20 (2011).
[6] S.-H. Oh, W. J. G. de Blok, E. Brinks, F. Walter, and J. Kennicutt, Robert C., Dark and luminous matter in THINGS dwarf galaxies, Astron. J. **141**, 193 (2011).
[7] S.-H. Oh, D. A. Hunter, E. Brinks, B. G. Elmegreen, A. Schruba, F. Walter, M. P. Rupen, L. M. Young, C. E. Simpson, M. C. Johnson, K. A. Herrmann, D. Ficut-Vicas, P. Cigan, V. Heesen, T. Ashley, and H.-X. Zhang, High-resolution mass models of dwarf galaxies from LITTLE THINGS, Astron. J. **149**, 180 (2015).
[8] J. F. Navarro, C. S. Frenk, and S. D. M. White, The structure of cold dark matter halos, Astrophys. J. **462**, 563 (1996).

[9] J. Wang, S. Bose, C. S. Frenk, L. Gao, A. Jenkins, V. Springel, and S. D. M. White, Universal structure of dark matter haloes over a mass range of 20 orders of magnitude, Nature (London) **585**, 39 (2020).

[10] J. F. Navarro, V. R. Eke, and C. S. Frenk, The cores of dwarf galaxy haloes, Mon. Not. R. Astron. Soc. **283**, L72 (1996).

[11] A. Pontzen and F. Governato, How supernova feedback turns dark matter cusps into cores, Mon. Not. R. Astron. Soc. **421**, 3464 (2012).

[12] A. Di Cintio, C. B. Brook, A. V. Macciò, G. S. Stinson, A. Knebe, A. A. Dutton, and J. Wadsley, The dependence of dark matter profiles on the stellar-to-halo mass ratio: A prediction for cusps versus cores, Mon. Not. R. Astron. Soc. **437**, 415 (2014).

[13] A. Benítez-Llambay, C. S. Frenk, A. D. Ludlow, and J. F. Navarro, Baryon-induced dark matter cores in the EAGLE simulations, Mon. Not. R. Astron. Soc. **488**, 2387 (2019).

[14] A. Lazar, J. S. Bullock, M. Boylan-Kolchin, T. K. Chan, P. F. Hopkins, A. S. Graus, A. Wetzel, K. El-Badry, C. Wheeler, M. C. Straight, D. Kereš, C.-A. Faucher-Giguère, A. Fitts, and S. Garrison-Kimmel, A dark matter profile to model diverse feedback-induced core sizes of ΛCDM haloes, Mon. Not. R. Astron. Soc. **497**, 2393 (2020).

[15] A. A. Dutton, T. Buck, A. V. Macciò, K. L. Dixon, M. Blank, and A. Obreja, NIHAO—XXV. Convergence in the cusp-core transformation of cold dark matter haloes at high star formation thresholds, Mon. Not. R. Astron. Soc. **499**, 2648 (2020).

[16] J. D. Burger and J. Zavala, Supernova-driven mechanism of Cusp-core Transformation: An appraisal, Astrophys. J. **921**, 126 (2021).

[17] S. Bose, C. S. Frenk, A. Jenkins, A. Fattahi, F. A. Gómez, R. J. J. Grand, F. Marinacci, J. F. Navarro, K. A. Oman, R. Pakmor, J. Schaye, C. M. Simpson, and V. Springel, No cores in dark matter-dominated dwarf galaxies with bursty star formation histories, Mon. Not. R. Astron. Soc. **486**, 4790 (2019).

[18] G. Kauffmann, Quantitative constraints on starburst cycles in galaxies with stellar masses in the range 10^8–10^{10} $M_\odot$, Mon. Not. R. Astron. Soc. **441**, 2717 (2014).

[19] D. R. Weisz, A. E. Dolphin, E. D. Skillman, J. Holtzman, K. M. Gilbert, J. J. Dalcanton, and B. F. Williams, The star formation histories of local group dwarf galaxies. I. Hubble space telescope/wide field planetary camera 2 observations, Astrophys. J. **789**, 147 (2014).

[20] N. Emami, B. Siana, D. R. Weisz, B. D. Johnson, X. Ma, and K. El-Badry, A closer look at bursty star formation with $L_{H\alpha}$ and L_{UV} distributions, Astrophys. J. **881**, 71 (2019).

[21] P. F. Hopkins, E. Quataert, and N. Murray, The structure of the interstellar medium of star-forming galaxies, Mon. Not. R. Astron. Soc. **421**, 3488 (2012).

[22] F. Marinacci, L. V. Sales, M. Vogelsberger, P. Torrey, and V. Springel, Simulating the interstellar medium and stellar feedback on a moving mesh: Implementation and isolated galaxies, Mon. Not. R. Astron. Soc. **489**, 4233 (2019).

[23] D. N. Spergel and P. J. Steinhardt, Observational Evidence for Self-Interacting Cold Dark Matter, Phys. Rev. Lett. **84**, 3760 (2000).

[24] M. Vogelsberger, J. Zavala, and A. Loeb, Subhaloes in self-interacting galactic dark matter haloes, Mon. Not. R. Astron. Soc. **423**, 3740 (2012).

[25] M. Rocha, A. H. G. Peter, J. S. Bullock, M. Kaplinghat, S. Garrison-Kimmel, J. Oñorbe, and L. A. Moustakas, Cosmological simulations with self-interacting dark matter—I. Constant-density cores and substructure, Mon. Not. R. Astron. Soc. **430**, 81 (2013).

[26] S. Tulin and H.-B. Yu, Dark matter self-interactions and small scale structure, Phys. Rep. **730**, 1 (2018).

[27] A. H. G. Peter, M. Rocha, J. S. Bullock, and M. Kaplinghat, Cosmological simulations with self-interacting dark matter—II. Halo shapes versus observations, Mon. Not. R. Astron. Soc. **430**, 105 (2013).

[28] M. Kaplinghat, S. Tulin, and H.-B. Yu, Dark Matter Halos as Particle Colliders: Unified Solution to Small-Scale Structure Puzzles from Dwarfs to Clusters, Phys. Rev. Lett. **116**, 041302 (2016).

[29] A. Robertson, R. Massey, and V. Eke, What does the Bullet Cluster tell us about self-interacting dark matter?, Mon. Not. R. Astron. Soc. **465**, 569 (2017).

[30] A. Robertson, D. Harvey, R. Massey, V. Eke, I. G. McCarthy, M. Jauzac, B. Li, and J. Schaye, Observable tests of self-interacting dark matter in galaxy clusters: Cosmological simulations with SIDM and baryons, Mon. Not. R. Astron. Soc. **488**, 3646 (2019).

[31] J. I. Read, M. G. Walker, and P. Steger, The case for a cold dark matter cusp in Draco, Mon. Not. R. Astron. Soc. **481**, 860 (2018).

[32] J. Zavala, M. Vogelsberger, and M. G. Walker, Constraining self-interacting dark matter with the Milky Way's dwarf spheroidals, Mon. Not. R. Astron. Soc. **431**, L20 (2013).

[33] J. Zavala, M. R. Lovell, M. Vogelsberger, and J. D. Burger, Diverse dark matter density at sub-kiloparsec scales in Milky Way satellites: Implications for the nature of dark matter, Phys. Rev. D **100**, 063007 (2019).

[34] See Supplemental Material at http://link.aps.org/supplemental/10.1103/PhysRevLett.129.191103 for further details on the numerical methods and extended background information, including Sec. IA, which contains Refs. [35–39], for a discussion of how the initial conditions are generated; Sec. IB, which contains additional Refs. [40–46], for further details on the simulation suite; Sec. IC for a description of how the simulated data are processed to produce the results presented here and the additional figures shown in the Supplemental Material itself; Sec. ID for a more detailed description of the resampling procedure presented on page 3; and Sec. II for a closer look at the shell formation mechanism. In particular, see Fig. 3 in the Supplemental Material for the projection of the shell feature into $|x| - v_y$ space.

[35] L. Hernquist, An analytical model for spherical galaxies and bulges, Astrophys. J. **356**, 359 (1990).

[36] V. Springel, T. Di Matteo, and L. Hernquist, Modelling feedback from stars and black holes in galaxy mergers, Mon. Not. R. Astron. Soc. **361**, 776 (2005).

[37] M. Asplund, N. Grevesse, A. J. Sauval, and P. Scott, The chemical composition of the sun, Annu. Rev. Astron. Astrophys. **47**, 481 (2009).

[38] A. S. Eddington, The distribution of stars in globular clusters, Mon. Not. R. Astron. Soc. **76**, 572 (1916).

[39] L. Hernquist, N-body realizations of compound galaxies, Astrophys. J. Suppl. Ser. **86**, 389 (1993).

[40] M. R. Krumholz and J. C. Tan, Slow star formation in dense gas: Evidence and implications, Astrophys. J. **654**, 304 (2007).
[41] S. Balberg, S. L. Shapiro, and S. Inagaki, Self-interacting dark matter halos and the gravothermal catastrophe, Astrophys. J. **568**, 475 (2002).
[42] P. Colín, V. Avila-Reese, O. Valenzuela, and C. Firmani, Structure and subhalo population of halos in a self-interacting dark matter cosmology, Astrophys. J. **581**, 777 (2002).
[43] J. Koda and P. R. Shapiro, Gravothermal collapse of isolated self-interacting dark matter haloes: N-body simulation versus the fluid model, Mon. Not. R. Astron. Soc. **415**, 1125 (2011).
[44] J. Pollack, D. N. Spergel, and P. J. Steinhardt, Supermassive black holes from ultra-strongly self-interacting dark matter, Astrophys. J. **804**, 131 (2015).
[45] H. Nishikawa, K. K. Boddy, and M. Kaplinghat, Accelerated core collapse in tidally stripped self-interacting dark matter halos, Phys. Rev. D **101**, 063009 (2020).
[46] C. Power, J. F. Navarro, A. Jenkins, C. S. Frenk, S. D. M. White, V. Springel, J. Stadel, and T. R. Quinn, The inner structure of Lambda CDM halos. 1. A Numerical convergence study, Mon. Not. R. Astron. Soc. **338**, 14 (2003).
[47] J. D. Burger, J. Zavala, L. V. Sales, M. Vogelsberger, F. Marinacci, and P. Torrey, Degeneracies between self-interacting dark matter and supernova feedback as cusp-core transformation mechanisms, Mon. Not. R. Astron. Soc. **513**, 3458 (2022).
[48] V. Springel and L. Hernquist, Cosmological smoothed particle hydrodynamics simulations: A hybrid multiphase model for star formation, Mon. Not. R. Astron. Soc. **339**, 289 (2003).
[49] V. Springel, E pur si muove: Galilieanan-invariant cosmological hydrodynamical simulations on a moving mesh, Mon. Not. R. Astron. Soc. **401**, 791 (2010).
[50] K. El-Badry, A. Wetzel, M. Geha, P. F. Hopkins, D. Kereš, T. K. Chan, and C.-A. Faucher-Giguère, Breathing FIRE: How stellar feedback drives radial migration, rapid size fluctuations, and population gradients in low-mass galaxies, Astrophys. J. **820**, 131 (2016).
[51] J. D. Burger and J. Zavala, The nature of core formation in dark matter haloes: Adiabatic or impulsive?, Mon. Not. R. Astron. Soc. **485**, 1008 (2019).
[52] J. Binney and S. Tremaine, *Galactic Dynamics: Second Edition* (Princeton University Press, Princeton, 2008).
[53] W. Dehnen and J. I. Read, N-body simulations of gravitational dynamics, Eur. Phys. J. Plus **126**, 55 (2011).
[54] A. M. Price-Whelan, D. W. Hogg, K. V. Johnston, M. K. Ness, H.-W. Rix, R. L. Beaton, J. R. Brownstein, D. A. García-Hernández, S. Hasselquist, C. R. Hayes, R. R. Lane, M. Shetrone, J. Sobeck, and G. Zasowski, Orbital torus imaging: Using element abundances to map orbits and mass in the milky way, Astrophys. J. **910**, 17 (2021).
[55] M. G. Walker, M. Mateo, and E. W. Olszewski, Stellar Velocities in the Carina, Fornax, Sculptor, and Sextans dSph Galaxies: Data From the Magellan/MMFS Survey, Astron. J. **137**, 3100 (2009).
[56] T. J. L. de Boer, E. Tolstoy, V. Hill, A. Saha, E. W. Olszewski, M. Mateo, E. Starkenburg, G. Battaglia, and M. G. Walker, The star formation and chemical evolution history of the Fornax dwarf spheroidal galaxy, Astron. Astrophys. **544**, A73 (2012).
[57] V. Rusakov, M. Monelli, C. Gallart, T. K. Fritz, T. Ruiz-Lara, E. J. Bernard, and S. Cassisi, The bursty star formation history of the Fornax dwarf spheroidal galaxy revealed with the HST, Mon. Not. R. Astron. Soc. **502**, 642 (2021).
[58] A. Genina, A. Benítez-Llambay, C. S. Frenk, S. Cole, A. Fattahi, J. F. Navarro, K. A. Oman, T. Sawala, and T. Theuns, The core-cusp problem: A matter of perspective, Mon. Not. R. Astron. Soc. **474**, 1398 (2018).
[59] R. E. Sanderson, A. Bellini, S. Casertano *et al.* (WFIRST Infrared Nearby Galaxies Survey (WINGS)), Astrometry with the Wide-Field Infrared Space Telescope, J. Astron. Telesc. Instrum. Syst. **5**, 044005 (2019).
[60] J. Simon, S. Birrer, K. Bechtol, S. Chakrabarti, F.-Y. Cyr-Racine, I. Dell'Antonio, A. Drlica-Wagner, C. Fassnacht, M. Geha, D. Gilman, Y. D. Hezaveh, D. Kim, T. S. Li, L. Strigari, and T. Treu, Testing the nature of dark matter with extremely large telescopes, Bull. Am. Astron. Soc. **51**, 153 (2019).
[61] M. C. Smith, G. L. Bryan, R. S. Somerville, C.-Y. Hu, R. Teyssier, B. Burkhart, and L. Hernquist, Efficient early stellar feedback can suppress galactic outflows by reducing supernova clustering, Mon. Not. R. Astron. Soc. **506**, 3882 (2021).